PLASTIC POLLUTION

Seafloor microplastic hotspots controlled by deep-sea circulation

Ian A. Kane[1]*, Michael A. Clare[2], Elda Miramontes[3,4], Roy Wogelius[1], James J. Rothwell[5], Pierre Garreau[6], Florian Pohl[7]

Although microplastics are known to pervade the global seafloor, the processes that control their dispersal and concentration in the deep sea remain largely unknown. Here, we show that thermohaline-driven currents, which build extensive seafloor sediment accumulations, can control the distribution of microplastics and create hotspots with the highest concentrations reported for any seafloor setting (190 pieces per 50 grams). Previous studies propose that microplastics are transported to the seafloor by vertical settling from surface accumulations; here, we demonstrate that the spatial distribution and ultimate fate of microplastics are strongly controlled by near-bed thermohaline currents (bottom currents). These currents are known to supply oxygen and nutrients to deep-sea benthos, suggesting that deep-sea biodiversity hotspots are also likely to be microplastic hotspots.

Plastic pollution has been observed in nearly all environments on Earth (*1*) and across all of its oceans (*2*–*4*). The effects of plastic pollution on marine ecosystems and implications for human health are of growing concern, as more than 10 million tonnes of plastic enter the global ocean each year (*4*–*6*). Converging surface currents in oceanic gyres are responsible for the global distribution of plastics on the ocean surface (*2*, *3*). These gyres effectively concentrate positively buoyant plastics into the now-infamous "garbage patches" (*2*, *3*). However, sea surface accumulations only account for ~1% of the estimated global marine plastic budget (*3*, *4*, *7*, *8*). Most of the remaining 99% of plastic ends up in the deep sea (*7*–*9*) (Fig. 1A). A considerable proportion [estimated at 13.5% (*8*)] of the marine plastic budget occurs as microplastics: small (<1 mm) fragments and fibers (*10*, *11*) that originate as manufactured particles (*12*, *13*) or are derived from synthetic textiles (*14*) or the breakdown of larger plastic debris (*15*). It has been shown that larger plastic debris may be associated with dense down-canyon flows in the Mediterranean (*16*). The seafloor is a globally important sink for plastics; however, the physical controls on the distribution of microplastics and the effectiveness of their sequestration once deposited at the seafloor remain unclear (*7*, *10*, *17*–*23*). Owing to their small size, microplastics can be ingested by organisms across all trophic levels, enabling transfer of harmful toxic substances (*9*, *10*, *22*). Therefore, determining where microplastics accumulate and their availability for incorporation into the food chain is fundamental to understanding threats to globally important deep-seafloor ecosystems (*24*).

Rather than corresponding to the extent of overlying surface garbage patches, microplastics on the deep seafloor are preferentially focused within distinct physiographic settings (*7*, *19*). Submarine canyons and deep-ocean trenches, which are foci for episodic yet powerful gravity flows, appear to be microplastic hotspots (*7*, *20*, *25*–*27*) (Fig. 2A). This physiographic bias suggests that the transfer of microplastics to and across the deep seafloor is therefore not solely explained by vertical settling from surface gyres. It is likely that the role of deep-sea currents in the dispersal and concentration of microplastics is similar to that of surface currents (*26*, *28*), yet a paucity of contextual data (e.g., bathymetric, oceanographic, and sedimentological) hinders the linkage of physical transport processes to the distribution and ultimate fate of microplastics. Thermohaline currents acting on the seafloor are one of the most important processes for the deep-sea transport of fine-grained particles and build some of the largest sediment accumulations on our planet [called contourite drifts (*29*)] (Fig. 1B), but their role in sequestering microplastics remains unknown.

Here, we link microplastic pollution on the seafloor to bottom currents by integrating high-resolution geophysical data, sediment sampling, microplastics analysis, and numerical modeling. The Tyrrhenian Sea was selected as the study area because (i) the dimensions and grain size of its physiographic elements are broadly comparable to those of many global settings (*29*–*32*); (ii) its ocean circulation patterns and velocities are comparable to currents globally (*31*, *33*); (iii) its plastic input volumes and locations are well constrained (*34*); and (iv) high-resolution seafloor and ocean circulation data afford the spatial and temporal context to investigate our key questions. We analyze data from the Tyrrhenian Sea, where ocean water circulation is driven by the East Corsican Current and its return branch (Figs. 1C and 2E), which reach local velocities of >0.4 m s^{-1} near the surface and >0.2 m s^{-1} near the seafloor (*30*). The strongest bottom currents generally occur between 600 and 900 m water depth, where they actively sculpt extensive muddy contourite drifts (Fig. 1D) [<10 km wide and up to hundreds of meters thick (*31*)]. The continental shelf is indented by the Caprera slope channel system, which extends downslope to the Olbia basin (*32*) (Fig. 1C). Terrestrial sediment is delivered to the shelf by high-gradient rivers passing through rural, urban, and industrial catchments and accounts for ~80% of the marine plastic budget in the region, with the remainder from shipping and fishing activities (*6*–*8*, *34*, *35*, *36*) (Fig. 1, A and C). In this study, we address three questions: How important are bottom currents for the dispersal and accumulation of microplastics on the deep seafloor? How do variations in bottom current intensity control the spatial distribution of microplastics at the seafloor? And how efficiently are microplastics sequestered after their emplacement at the seafloor?

All seafloor samples were found to contain microplastics (Fig. 3B and table S1), as verified with optical microscopy and Fourier transform infrared (FTIR) spectroscopy (fig. S2). Microplastics presented in two forms, as fibers (70 to 100%) and as fragments (0 to 30%) (Fig. 2, B and C). Microplastic concentration in the Tyrrhenian Sea includes the highest values yet recorded from the deep seafloor (Fig. 2A): up to 182 fibers and nine fragments per 50 g of dried sediment (191 total pieces per 50 g in core 6, equivalent to ~1.9 million pieces per square meter) were recorded in the contourite drift at the base of the northeast Sardinian continental slope (Fig. 3, B and C). This concentration exceeds the highest levels previously recorded, including those from deep-sea trenches, and is more than double that documented in submarine canyons (*27*, *37*–*39*) (Fig. 2A). As contourite drifts occur on most of Earth's continental margins (*29*) (Fig. 1B), the high concentrations recorded here strongly suggest that these drifts are globally important repositories for microplastics.

In our study area there is no relationship between microplastic concentrations and distance from terrestrial plastic sources (Fig. 2B). Samples from the continental shelf (38 fibers and 3 fragments; core 9) and upper slope (8 fibers and 1 fragment; core 11) have some of the lowest concentrations reported in the study area. Instead, we show that microplastics are focused within a water depth range of

[1]School of Earth and Environmental Sciences, University of Manchester, Manchester M13 9PL, UK. [2]National Oceanography Centre, University of Southampton Waterfront Campus, Southampton SO14 3ZH, UK. [3]Faculty of Geosciences, University of Bremen, 28359 Bremen, Germany. [4]MARUM-Center for Marine Environmental Sciences, University of Bremen, 28359 Bremen, Germany. [5]Department of Geography, University of Manchester, Manchester M13 9PL, UK. [6]IFREMER, Univ. Brest, CNRS UMR 6523, IRD, Laboratoire d'Océanographie Physique et Spatiale (LOPS), IUEM, 29280, Plouzané, France. [7]Department of Earth Sciences, Durham University, Durham DH1 3LE, UK.
*Corresponding author. Email: ian.kane@manchester.ac.uk

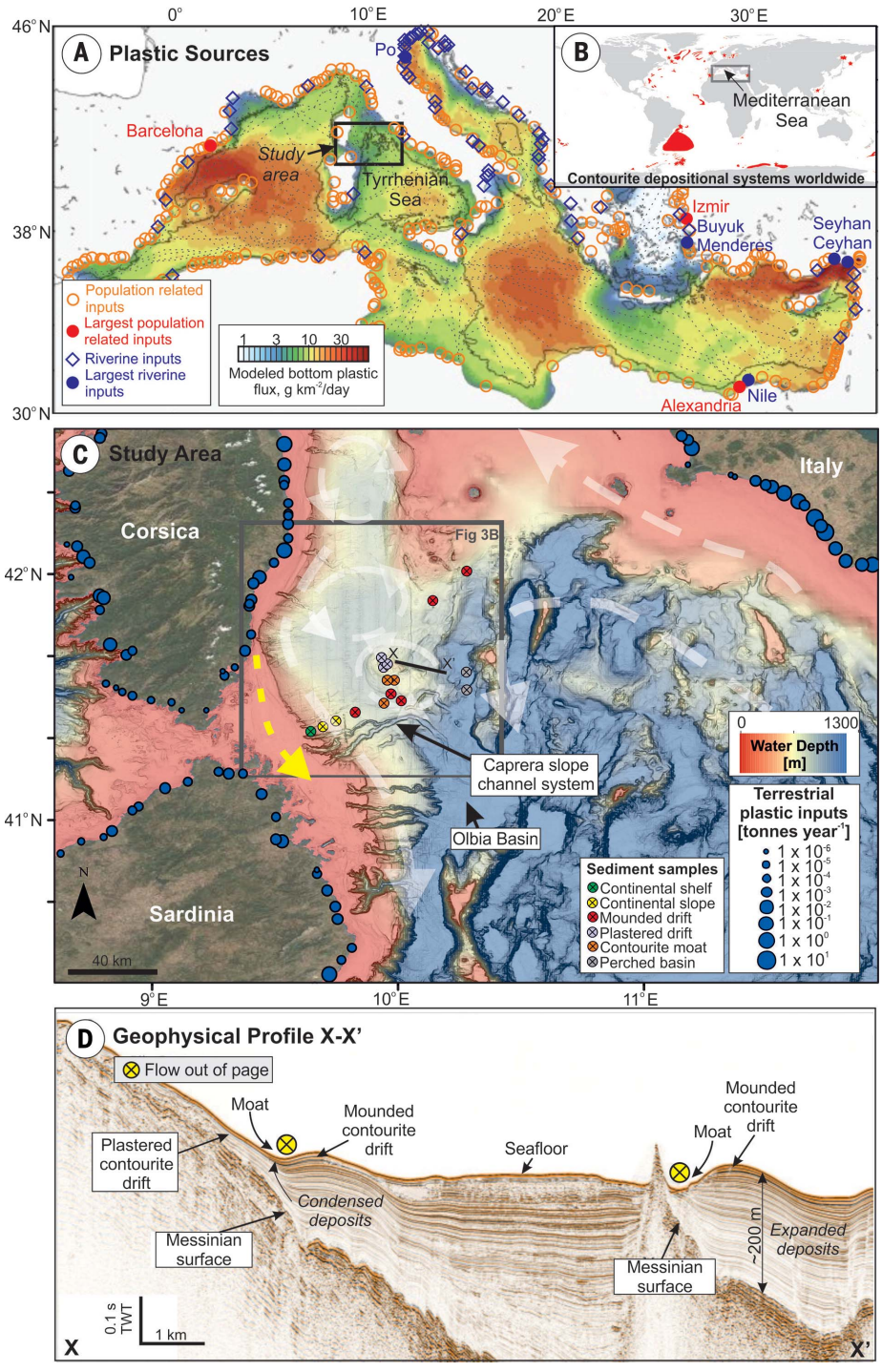

Fig. 1. Plastic sources and ocean circulation affecting the Tyrrhenian Sea. (**A**) Location of study area in the Tyrrhenian Sea, annotated with published terrestrial (~80%) and maritime (fishing and shipping; ~20%) plastic sources (*34*). Terrestrial input sources shown as circles and diamonds. Vessel traffic and shipping lanes shown as dashed lines. Modeled (and hence inferred) plastic debris fluxes on the Mediterranean seafloor illustrated as colored shading. The period modeled was 2013–2017, assuming vertical settling from surface distributions using a two-dimensional Lagrangian model (*34*). Inferred values in the northern Tyrrhenian Sea are <7 g km^{-2} day^{-1}, which are low compared with those of the wider Mediterranean Sea. (**B**) Global distribution of documented contourite depositional systems (*29*) shown in red. (**C**) Seafloor bathymetry of the northern Tyrrhenian Sea annotated with documented terrestrial plastic input sources (*6*), named physiographic features (*32*), and seafloor sediment samples analyzed in this study (colored according to physiographic domain). The regional pattern of thermohaline-driven currents near the seafloor is shown by white arrows. Along-shore drift on the Corsican and Sardinian continental shelves is shown by a yellow dashed arrow. Line X–X′ shows the location of the multichannel seismic line in (**D**), which illustrates the depositional features that have developed as a result of bottom currents, including the formation of thick mounded drifts, and inhibited sediment accumulation in moats. TWT, two-way travel time.

600 to 900 m, where bottom currents form seafloor gyres and have the greatest interaction with the seafloor (Fig. 2C). The influence of these currents and the complex topographic relief (Fig. 2E) result in spatial variations in the shear stress exerted on the seafloor, as determined from hydrodynamic modeling (Fig. 3B). These variations in shear stress explain the localized seafloor distribution of microplastic particles, which typically have lower densities than silt- and sand-forming minerals and therefore are more easily entrained (*39*), accounting for depleted levels of microplastic in certain physiographic domains and concentration in others (Figs. 2D and 3C). The lowest concentrations of microplastics are found in contour-parallel moats, which are foci for erosion and/or nondeposition (e.g., 28 fibers and 3 fragments per 50 g in core 16) (Fig. 3C). Higher concentrations occur on the adjacent mounded drift (e.g., 86 fibers and 1 fragment in core 8) and also in other mounded drift accumulations (e.g., 88 fibers and 6 fragments in core 2) (Fig. 3, B and C).

Although microplastic abundance is generally higher where bottom currents occur, it appears that there is a threshold bed shear stress above which microplastics no longer become concentrated at the seafloor. Modeling of particle transport under the ranges of shear stresses determined from the hydrodynamic model indicates that microplastics are likely to be remobilized and potentially

transported as bedload at shear stresses in excess of 0.03 to 0.04 N m^{-2} (Figs. 3A and 4). Areas of higher shear stress are observed on the shelf break, upper continental slope, and particularly in contourite moats, where the bottom current is most vigorous (Fig. 3B). We propose that such contour currents are effective agents for the transport of microplastics and that, while microplastics are generally flushed along-slope through contourite moats, they preferentially accumulate in the adjacent contourite drifts, forming anomalously concentrated microplastic hotspots. This appears to be particularly true for mounded contourite drifts, which are often sites of extremely high sediment accumulation relative to the rest of a continental slope (*29*).

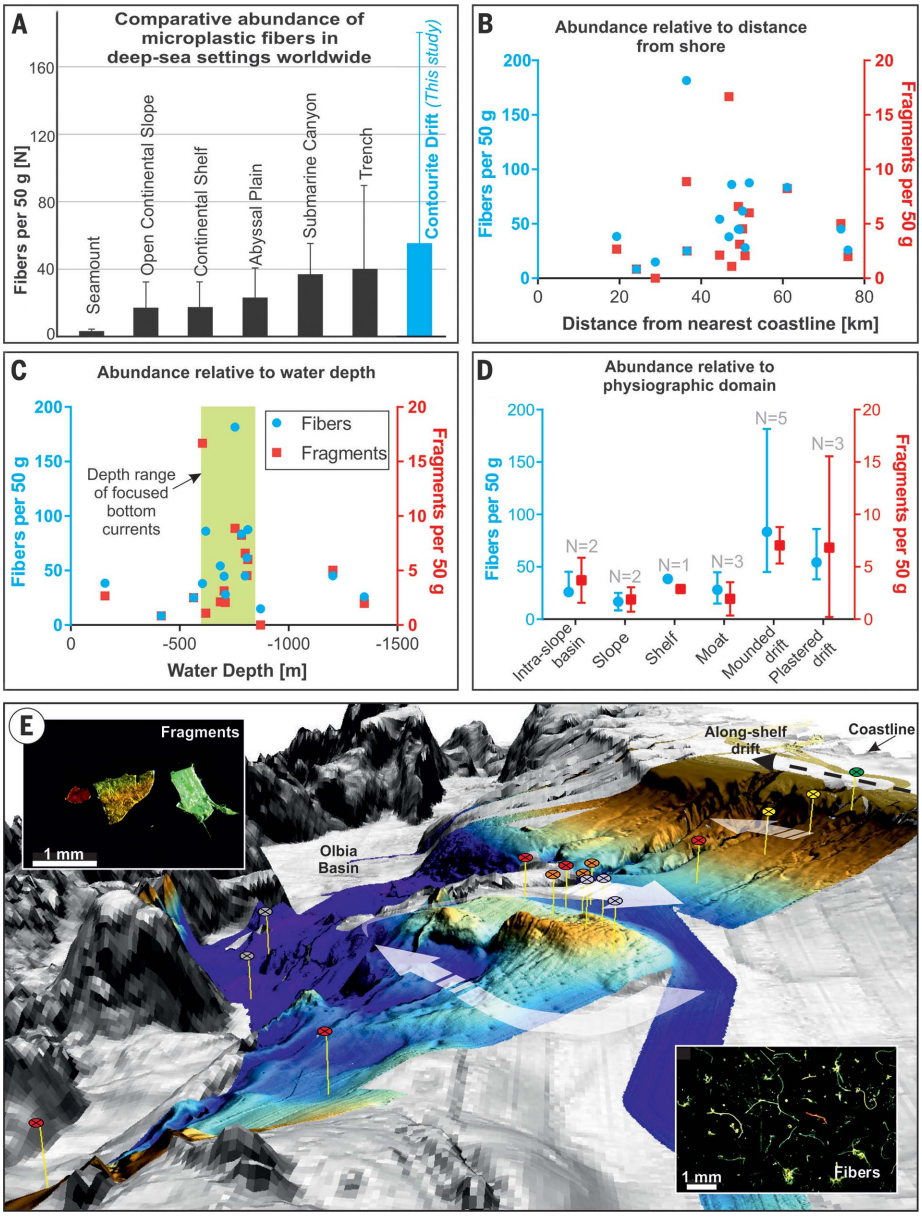

Fig. 2. Global and local abundance of seafloor microplastics. (**A**) Comparison of microplastic fiber abundance in different deep-sea settings worldwide (see supplementary materials), demonstrating the high concentrations observed in the contourite drift deposits in the Tyrrhenian Sea. (**B** to **D**) Results from the Tyrrhenian Sea illustrating that (B) microplastic abundance does not decrease with distance from terrestrial input sources, (C) microplastics appear to be concentrated within a depth range of ~600 to 900 m, and (D) microplastic concentration is biased toward physiographic domains, particularly mounded drifts, and depleted within moats. (**E**) A three-dimensional rendering (perspective view looking toward the southwest) of the regional European Marine Observation and Data Network (EMODNet) bathymetry (grayscale) and autonomous underwater vehicle (AUV) bathymetry (colored) shows the relationship of sediment samples to the local seafloor currents (10× vertical exaggeration). Horizontal distance from bottom left core (red circle) to top left (green circle) is ~100 km. Compare to map view in Fig. 1C. Inset microscope photographs show representative examples of fibers and fragments extracted from the sediment.

Previous Lagrangian modeling of microplastic transport in the Mediterranean [based on a model used to describe global microplastic distributions (*3*)] suggests that waves and sea-surface currents ought to transport microplastics away from the Tyrrhenian Sea (*34*). Therefore, the bottom plastic flux (assuming vertical settling only) in this basin should be one of the lowest: 1.5 to 7 g km^{-2} day^{-1}, compared with a regional maximum of 70 g km^{-2} day^{-1} elsewhere in the Mediterranean (Fig. 1A). If that modeling is correct, microplastic abundances elsewhere in the Mediterranean may be even higher than the values we report here. We suggest, however, that both bottom currents and surface currents are important for the concentration of microplastics, yet near-bed bottom-current circulation is omitted from existing models (*2*, *3*, *8*, *34*). Ocean currents appear to be highly capable of diverting microplastics from shallow to deep water and may be responsible for entraining microplastics transported downslope via submarine channels linked to terrestrial sources (Fig. 5). In enclosed or semienclosed basins, such as the Tyrrhenian Sea and more widely the Mediterranean Sea, circulating contour currents are likely to preferentially accumulate microplastics within contourite drifts. On open continental slopes, contour currents may disperse rather than concentrate microplastics. In such settings, these currents may play a key role in their spatial segregation into hotspots.

We have shown that the overall pattern of bottom currents controls the distribution of microplastics at the seafloor. Numerical modeling and direct measurements in the Tyrrhenian Sea reveal a pronounced seasonal variation in bottom current velocities, with bottom currents being most intense in the winter (*31*). Modeling of microplastic transport shows that some of the near-bed bottom current shear stresses are close to, or in excess of, that required to entrain both fibers and fragments (Figs. 3A and 4). Although low-intensity currents in the summer may allow for the accumulation of microplastics at the seafloor, at some locations (contourite moats, in particular), previously deposited microplastics may be reexhumed as shear stresses exceed the critical boundary for remobilization and suspension (Fig. 3A). More powerful but ephemeral seafloor flows such as gravity currents that have been recorded in deep-sea submarine canyons can reach velocities two orders of magnitude greater than those of the bottom currents in the Tyrrhenian Sea (up to 20 m s^{-1}) and can last for several days (*40*–*42*). These powerful events will undoubtedly flush accumulated microplastics either farther downslope (*43*) or loft them for recirculation by

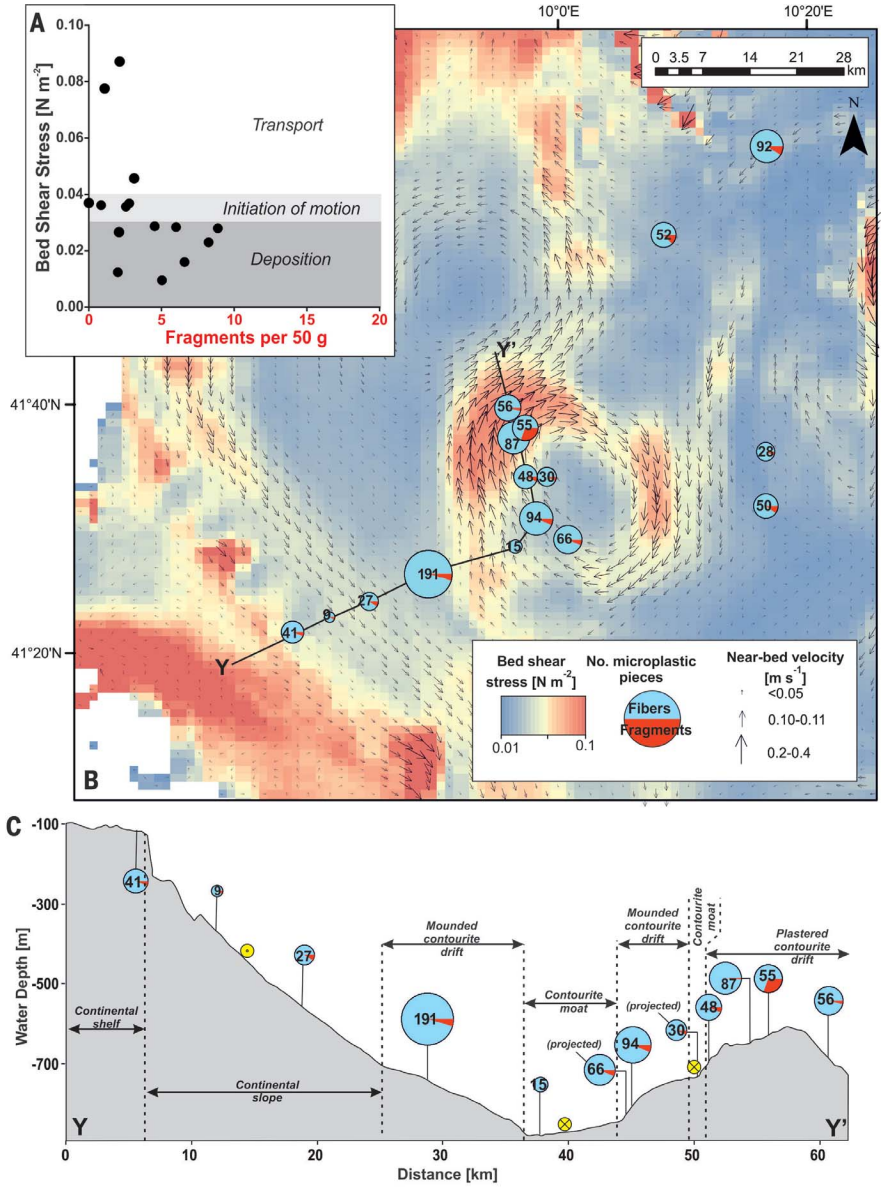

Fig. 3. Influence of bottom currents on the distribution of seafloor microplastics. (**A**) As near-bed shear stresses initially increase, so does the concentration of microplastics; however, when a threshold (~0.04 N m^{-2}) is exceeded, there is a sudden reduction in the abundance of microplastics. This corresponds to the modeled threshold of motion based on empirical approaches (Fig. 4 and fig. S6). (**B**) Hydrodynamic modeling of bottom current circulation shows the formation of seafloor gyres, with corridors of enhanced bed shear stress along the continental slope that are particularly focused within contourite moats and on the flanks of a prominent seamount. Ninetieth percentile for bed shear stress and mean near-bed (bottom current) velocity are shown (see supplementary materials). This focusing of bottom current intensity explains the limited abundance of microplastics on the shelf, upper continental slope, and within contourite moats. (**C**) Zones of lower shear stresses adjacent to these corridors of elevated currents (where mounded contourite drifts form) feature the highest concentrations of microplastics.

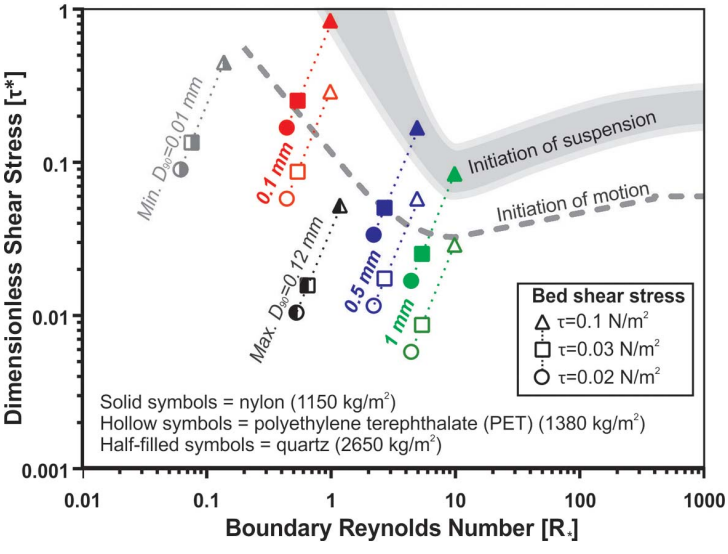

Fig. 4. Relating microplastics to seafloor shear stress. Flow regime diagram to show that the critical shear stress required to move particles [i.e., above the dashed gray line (*51*)] falls between 0.03 and 0.04 N m^{-2}, and that suspension [i.e., within or above the gray shaded area (*52*, *53*)] may occur >0.1 N m^{-2}. Two densities of microplastics are assumed (nylon and polyethylene) on the basis of the results of FTIR analysis. Three particle sizes for microplastics are shown, to represent the general range observed through visual microscopic examination [0.1 mm (red symbols), 0.5 mm (blue), and 1 mm (green) width]. The upper and lower bound measured grain sizes (D_{90}) for the host sediment are also shown with gray symbols.

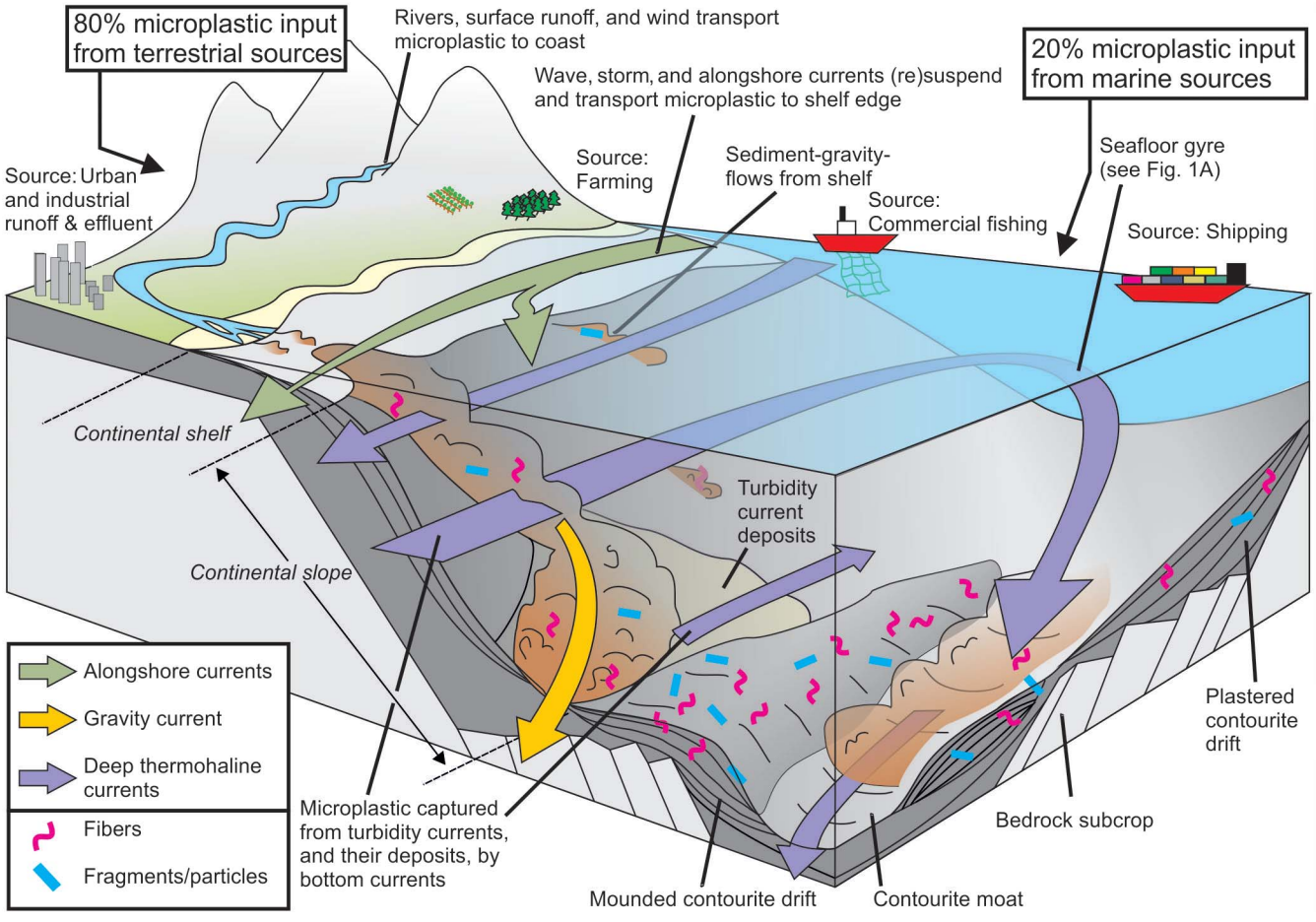

Fig. 5. Bottom currents control the deep-sea fate of microplastics. Schematic diagram illustrating the role of near-bed currents in the transfer, concentration, and storage of microplastics in the deep sea. Along-shelf currents disperse microplastics, powerful gravity flows effectively flush microplastics to the deep sea, while thermohaline-driven bottom currents segregate microplastics into localized hotspots of high concentration. The effectiveness of their long-term sequestration depends on the intensity of subsequent bottom current activity and rate of burial.

thermohaline bottom currents (Fig. 5). Such gravity flows play a globally important role in the lateral transport of lightweight particulate matter such as organic carbon (*41*, *44*); hence, it stands to reason that they should also be important for microplastic transport. Episodic flushing of submarine canyons (*41*, *42*, *45*) suggests that canyons may only be temporary microplastic storage sites (*26*). This is analogous to rivers where flooding can flush high levels of microplastics downstream (*46*).

Bottom currents are efficient conveyors of nutrients and oxygen, and consequently they dictate the location of important biodiversity hotspots (*41*, *47*–*49*). Unfortunately, we show that the same seafloor currents can also transport and emplace microplastics. The highest concentrations of microplastics on the seafloor occur in contourite drifts formed by bottom currents, and their distribution is controlled by spatial variations in current intensity. How effectively microplastics are buried or become reexhumed (and hence become more available for trophic transfer) depends on temporal fluctuations in current intensity. Although there are ongoing efforts to reduce the release of plastics into the environment, our oceans will continue to be affected by the legacy of past waste mismanagement (*4*, *5*, *8*, *50*). Seafloor currents will play a crucial role in the future transfer and storage of microplastics in the deep ocean.

REFERENCES AND NOTES

1. M. L. Taylor, C. Gwinnett, L. F. Robinson, L. C. Woodall, *Sci. Rep.* **6**, 33997 (2016).
2. M. Eriksen *et al.*, *PLOS ONE* **9**, e111913 (2014).
3. E. van Sebille *et al.*, *Environ. Res. Lett.* **10**, 124006 (2015).
4. J. R. Jambeck *et al.*, *Science* **347**, 768–771 (2015).
5. R. Geyer, J. R. Jambeck, K. L. Law, *Sci. Adv.* **3**, e1700782 (2017).
6. L. C. M. Lebreton *et al.*, *Nat. Commun.* **8**, 15611 (2017).
7. R. C. Thompson *et al.*, *Science* **304**, 838–838 (2004).
8. A. A. Koelmans, M. Kooi, K. L. Law, E. van Sebille, *Environ. Res. Lett.* **12**, 114028 (2017).
9. C. A. Choy *et al.*, *Sci. Rep.* **9**, 7843 (2019).
10. L. Van Cauwenberghe, L. Devriese, F. Galgani, J. Robbens, C. R. Janssen, *Mar. Environ. Res.* **111**, 5–17 (2015).
11. A. Vianello *et al.*, *Estuar. Coast. Shelf Sci.* **130**, 54–61 (2013).
12. V. Zitko, M. Hanlon, *Mar. Pollut. Bull.* **22**, 41–42 (1991).
13. S. A. Mason *et al.*, *Environ. Pollut.* **218**, 1045–1054 (2016).
14. M. A. Browne *et al.*, *Environ. Sci. Technol.* **45**, 9175–9179 (2011).
15. A. L. Andrady, *Mar. Pollut. Bull.* **62**, 1596–1605 (2011).
16. X. Tubau *et al.*, *Prog. Oceanogr.* **134**, 379–403 (2015).
17. E. D. Goldberg, *Environ. Technol.* **18**, 195–201 (1997).
18. A. Ballent, A. Purser, P. de Jesus Mendes, S. Pando, L. Thomsen, *Biogeosciences Discuss.* **9**, 18755–18798 (2012).
19. C. K. Pham *et al.*, *PLOS ONE* **9**, e95839 (2014).
20. L. C. Woodall *et al.*, *R. Soc. Open Sci.* **1**, 140317 (2014).
21. V. Fischer, N. O. Elsner, N. Brenke, E. Schwabe, A. Brandt, *Deep Sea Res. Part II Top. Stud. Oceanogr.* **111**, 399–405 (2015).
22. W. Courtene-Jones, B. Quinn, S. F. Gary, A. O. M. Mogg, B. E. Narayanaswamy, *Environ. Pollut.* **231**, 271–280 (2017).
23. A. J. Underwood, M. G. Chapman, M. A. Browne, *Anal. Methods* **9**, 1332–1345 (2017).
24. A. R. Thurber *et al.*, *Biogeosciences* **11**, 3941–3963 (2014).
25. D. K. Barnes, F. Galgani, R. C. Thompson, M. Barlaz, *Philos. Trans. R. Soc. London Ser. B* **364**, 1985–1998 (2009).
26. A. Ballent, S. Pando, A. Purser, M. F. Juliano, L. Thomsen, *Biogeosciences* **10**, 7957–7970 (2013).
27. X. Peng *et al.*, *Geochem. Perspect. Lett.* **9**, 1–5 (2018).
28. I. E. Chubarenko *et al.*, in *Microplastic Contamination in Aquatic Environments* (Elsevier, 2018), pp. 175–223.
29. M. Rebesco, F. J. Hernández-Molina, D. Van Rooij, A. Wåhlin, *Mar. Geol.* **352**, 111–154 (2014).
30. S. Vignudelli, P. Cipollini, M. Astraldi, G. P. Gasparini, G. Manzella, *J. Geophys. Res. Oceans* **105**, 19649–19663 (2000).

31. E. Miramontes *et al*., *Geomorphology* **333**, 43–60 (2019).
32. G. Dalla Valle, F. Gamberi, *Mar. Geol.* **286**, 95–105 (2011).
33. I. N. McCave, *Mar. Geol.* **390**, 89–93 (2017).
34. S. Liubartseva, G. Coppini, R. Lecci, E. Clementi, *Mar. Pollut. Bull.* **129**, 151–162 (2018).
35. C. Cencini, *J. Coast. Res.* **14**, 774–793 (1998).
36. D. A. Kroodsma *et al*., *Science* **359**, 904–908 (2018).
37. M. Bergmann *et al*., *Environ. Sci. Technol.* **51**, 11000–11010 (2017).
38. A. Sanchez-Vidal, R. C. Thompson, M. Canals, W. P. de Haan, *PLOS ONE* **13**, e0207033 (2018).
39. I. A. Kane, M. A. Clare, *Front. Earth Sci.* **7**, 80 (2019).
40. D. J. Piper, P. Cochonat, M. L. Morrison, *Sedimentology* **46**, 79–97 (1999).
41. M. Azpiroz-Zabala *et al*., *Sci. Adv.* **3**, e1700200 (2017).
42. J. J. Mountjoy *et al*., *Sci. Adv.* **4**, eaar3748 (2018).
43. F. Pohl, J. T. Eggenhuisen, I. A. Kane, M. A. Clare, *Environ. Sci. Technol.* **54**, 4180–4189 (2020).
44. V. Galy *et al*., *Nature* **450**, 407–410 (2007).
45. M. Canals *et al*., *Nature* **444**, 354–357 (2006).
46. R. Hurley, J. Woodward, J. J. Rothwell, *Nat. Geosci.* **11**, 251–257 (2018).
47. S. J. Hall, *Environ. Conserv.* **29**, 350–374 (2002).
48. C. Treignier, S. Derenne, A. Saliot, *Org. Geochem.* **37**, 1170–1184 (2006).
49. A. J. Davies *et al*., *Limnol. Oceanogr.* **54**, 620–629 (2009).
50. D. Xanthos, T. R. Walker, *Mar. Pollut. Bull.* **118**, 17–26 (2017).
51. A. Shields, thesis, Technische Universität Berlin (Preussischen Versuchsanstalt für Wasserbau, 1936).
52. L. C. van Rijn, *J. Hydraul. Eng.* **110**, 1613–1641 (1984).
53. Y. Niño, F. Lopez, M. Garcia, *Sedimentology* **50**, 247–263 (2003).
54. I. Kane *et al*., Data from: Seafloor microplastic hotspots controlled by deep-sea circulation, Dryad (2020); https://doi.org/10.5061/dryad.tht76hdwf.

ACKNOWLEDGMENTS

We thank T. Bishop and J. Moore in the Department of Geography at the University of Manchester for help with a range of analyses. We thank the staff at the British Ocean Sediment Core Research Facility (BOSCORF) for access to sediment cores. We thank the GALSI PROJECT for access to survey data. The constructive comments of D. Piper and two anonymous reviewers are gratefully acknowledged. **Funding:** M.A.C. was supported by the CLASS program (NERC grant NE/R015953/1). **Author contributions:** I.A.K. and M.A.C. conceived of and designed the study and subsampled the core samples. I.A.K. carried out the microplastic extraction and analysis. M.A.C. and I.A.K. analyzed seafloor and subsurface data and integrated microplastics concentrations with modeling outputs. E.M. and P.G. modeled the seafloor circulation patterns. F.P. integrated microplastic and sediment transport modeling work. R.W. analyzed FTIR spectra. All authors contributed to writing the manuscript. **Competing interests:** The authors declare no competing interests. **Data and materials availability:** The data that support the findings of this study are available from Dryad (*54*).

SUPPLEMENTARY MATERIALS

science.sciencemag.org/content/368/6495/1140/suppl/DC1
Materials and Methods
Figs. S1 to S5
Table S1
References (*55*–*72*)
Data S1

16 December 2019; accepted 9 April 2020
Published online 30 April 2020
10.1126/science.aba5899